Optics Communications 281 (2008) 5382–5384

Contents lists available at ScienceDirect

Optics Communications

journal homepage: www.elsevier.com/locate/optcom

High-power passive mode-locking of a diode pumped Yb:$GdVO_4$ laser

H. Luo [a,d,*], D.Y. Tang [a], G.Q. Xie [a,d], H.J. Zhang [b], L.J. Qin [c], H.H. Yu [b], L.Y. Ng [a], L.J. Qian [d]

[a] School of Electrical and Electronic Engineering, Nanyang Technological University, Singapore 639798, Singapore
[b] National Key Laboratory of Crystal Materials, Shandong University, Jinan 250100, China
[c] College of Environment and Material Engineering, Yantai University, Yantai 264005, China
[d] Research Facility for Advanced Materials, State Key Laboratory for Advanced Photonic Materials and Devices, Department of Optical Science and Engineering, Fudan University, Shanghai 200433, China

ARTICLE INFO

Article history:
Received 21 April 2008
Received in revised form 20 June 2008
Accepted 21 July 2008

ABSTRACT

Passive mode-locking of a diode pumped Yb-doped $GdVO_4$ crystal laser was demonstrated for the first time to our knowledge. The laser was mode-locked at the wavelength of 1019.1 nm and had an average output power of 1.01 W. The mode-locked pulse duration was 3.1 ps. The laser was end-pumped by a high-power fiber pigtailed laser diode bar and the mode-locking was enabled by a semiconductor saturable absorber mirror (SESAM).

1. Introduction

Yb-doped laser materials have attracted considerable attention over the past decade [1–8]. Yb^{3+} has a very simple electronic structure based on only two manifolds, which ensures few quantum defects and no parasitic levels. The low quantum defect of the ion (generally less than 5%) reduces the thermal load and thus thermal problems, and the absence of parasitic levels eliminates undesired effects such as the excited state absorption, up conversion, and concentration quenching. Moreover, the Yb-doped materials have a broad absorption band ranging from 940 to 985 nm, which matches with the emission wavelength of the InGaAs laser diodes, permitting direct diode pumping. Laser operation of various Yb-doped materials has been extensively investigated.

Vanadate crystals including YVO_4, $GdVO_4$, and $LuVO_4$ have been proven to be excellent laser host for high efficient laser emission. Yb^{3+}-doped vanadate crystals exhibit broad gain bandwidth, which is also attractive for the diode pumped ultrashort pulse solid-state lasers. Recently, passive mode-locking of the diode pumped Yb:YVO_4 lasers either using the Kerr-lens technique or the SESAM method has been demonstrated [2,9]. However, to the best of our knowledge, no mode-locking of the diode pumped Yb:$GdVO_4$ lasers has been reported. Compared with the Yb-doped YVO_4 crystal, although the Yb-doped $GdVO_4$ crystal has slightly smaller stimulated cross-sections, it has larger thermal conductivities along the *a*-axis (7.1 $W\,m^{-1}\,K^{-1}$) and *c*-axis (8.1 $W\,m^{-1}\,K^{-1}$) [1,10], which permits high power mode-locked laser operation. CW laser oscillation in Yb:$GdVO_4$ was first demonstrated using Ti:sapphire laser pumping, attained an output power of 420 mW [1]. A recent work employing high-power diode pumping of Yb:$GdVO_4$ has achieved a cw output power as high as 4.0 W [4]. In this paper, we demonstrate for the first time passive mode-locking of a Yb:$GdVO_4$ laser end-pumped by a fiber pigtailed laser diode bar, yielding 1.01-W average output power.

2. Experimental setup

The Yb:$GdVO_4$ crystal used in the laser was grown by the Czochralski method. It has a Yb-doping concentration of 0.8 at.%. The Yb:$GdVO_4$ crystal has a dimension of 3 mm × 3 mm in cross-section and 3.18 mm in length. Both sides of the crystal were AR-coated in a broad band from 1020 to 1110 nm at normal incidence. The absorption peak of the Yb:$GdVO_4$ crystal locates at ∼985 nm at room temperature [1,4]. In order to remove the generated heat in the crystal for effective laser operation, the crystal was wrapped in indium foil and mounted tightly in a water-cooled copper holder that is maintained at a temperature of 9 °C. It was observed that the cw mode-locking lost its long-term stability with the absence of water cooling. The water cooling is also to avoid possible damage of the crystal from high temperature. A 25-W fiber coupled laser diode bar (LIMO GmbH, LIMO25-F100-DL980) was used as the pump source. The core size of the fiber was 50 μm in radius, with a numerical aperture of 0.22. The center emission wavelength of the diode shifted between 972 and 977 nm depending on the output power level. No extra means was applied to control the pumping wavelength. The pump beam from the fiber was focused by two 1:1 reimaging lenses of 2 cm focal length. The focal spot in the Yb:$GdVO_4$ had a radial size of ∼50 μm.

For the mode-locked laser operation, a folded laser cavity was used as schematically shown in Fig. 1. The cavity consisted of a SESAM, an output coupler (OC), and two mirrors M1 and M2. Flat mirror M1 was the pump input mirror. It has high transmission

* Corresponding author. Address: School of Electrical and Electronic Engineering, Nanyang Technological University, Singapore 639798, Singapore.
E-mail address: luohang@fudan.edu.cn (H. Luo).

0030-4018/$ - see front matter © 2008 Elsevier B.V. All rights reserved.
doi:10.1016/j.optcom.2008.07.039

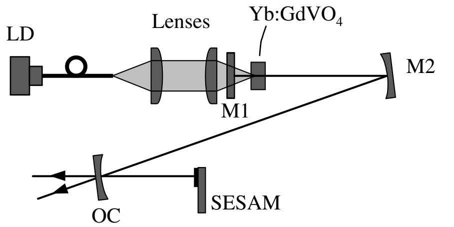

Fig. 1. Experimental setup for the mode-locked $Yb:GdVO_4$ laser. M1 and M2, mirrors. OC, output coupler.

in a band between 500 and 985 nm and high reflection in a broad bandwidth from 1020 to 1100 nm. A concave mirror M2 ($R = -200$ mm) had high reflection in a broad band from 1020 to 1100 nm. A plano-concave ($R = -50$ mm) OC mirror with transmission $T = 6\%$ was used. The length between M1 and M2 was ~100 mm, and the length between OC and SESAM was ~50 mm, while M2 and OC were separated by ~963 mm. The total cavity length added up to 1113 mm. The SESAM (BATOP GmbH, SAM-1040-1) used in our experiment has a central absorption wavelength of 1040 nm and 1% initial absorption strength. The modulation depth of the SESAM was 0.5%. The relaxation time was ~500 fs and the saturation fluence was 90 $\mu J/cm^2$. The SESAM was mounted on a copper holder. The laser cavity was designed to get a laser beam diameter of ~50 μm in the crystal to match with the pump beam, and ~10 μm on the SESAM. No dispersion compensation element, e.g., intracavity prisms, was applied. The mode-locked pulse train generated was detected with a fast photoreceiver (New Focus Inc. 1611-FS) with a rising time of 400 ps and plotted onto a digital oscilloscope (DPO7104, Tektroniks, bandwidth 1 GHz, 20 GS/s). Spectra and autocorrelation traces of the mode-locked pulses were measured with an optical spectrum analyzer (ANDO AQ-6315) and a commercial autocorrelator (Femtochrome Research, Inc. FR-103XL).

3. Results and discussion

Fig. 2 shows the experimentally measured mode-locked pulse trains. Stable cw mode-locking was established above an absorbed pump power of 5.18 W. Fig. 2a and b shows the pulse trains of stable cw mode-locking in 10 μs and 500 ns scales, respectively. As the absorbed pump power fell below 5.18 W, the laser pulses switched to CW mode-locking regime. Fig. 2c shows Q-switched mode-locked pulse trains at an absorbed pump power level below 5.18 W. At the maximum absorbed pump power of 7.6 W available in our experiment, the average output power attained 1.01 W, with an optical–optical conversion efficiency of 13.2%. The slope efficiency was 25.1% (Fig. 3a). This compared to an optical–optical conversion efficiency of 38.9% and a slope efficiency of 50.6% in a cw operation setup with a simple two-mirror cavity configuration (Fig. 3b). The cw mode-locked pulses repetition rate was 134.8 MHz and pulse-to-pulse intensity fluctuation was ~2.3%. Under stable mode-locking, the laser emitted in good TEM_{00} transverse mode. Because Yb-doped materials have long excited-state lifetimes, the cw mode-locked laser had a strong tendency to fall into Q-switching or Q-switched mode-locking regime when threshold condition for stable cw mode-locking is not satisfied. As a result, precise alignment of the cavity was required to produce a proper intracavity laser beam spot-size diameter on the SESAM in order to reduce the pump threshold to suppress Q-switching and enable stable cw mode-locking. Also the cavity should be properly adjusted to eliminate high-order transverse modes and ensure TEM_{00} mode operation.

We analyzed the threshold condition on the intracavity laser pulse energy for stable cw mode-locking of the laser. With a SESAM as mode-locker, the threshold of intracavity laser pulse energy is determined approximately by Honninger et al. [11]

$$E_p = (E_{sat,L} E_{sat,A} \lambda R)^{1/2} \tag{1}$$

where $E_{sat,L}$ is the saturation energy of the gain, $E_{sat,A}$ denotes the saturation energy of absorber, and ΔR denotes the maximum modulation depth of the SESAM. $E_{sat,L}$ is defined as the product of saturation fluence $F_{sat,A} = h\nu/(m\sigma_L)$ and the effective laser mode area inside the gain medium, where m is the number of passes through the gain element per cavity round trip and σ_L is the emission cross-section of the gain medium. $E_{sat,A}$ is defined by the product of absorber saturation fluence $F_{sat,A}$ and effective laser mode area on the saturable absorber. With modulation depth $\Delta R \sim 0.5\%$ and saturation fluence ~90 $\mu J/cm^2$ of the SESAM used, and with $\sigma_L \sim 0.5 \times 10^{-20}\ cm^2$ at 1019.1 nm [4], we estimated the threshold intracavity pulse energy for stable cw mode-locking to be ~47 nJ in our experiment. This calculated result coincides with the measured intracavity pulse energy threshold of 53 nJ, at absorbed pump level of 5.18 W. According to Eq. (1), there are possible ways to reduce

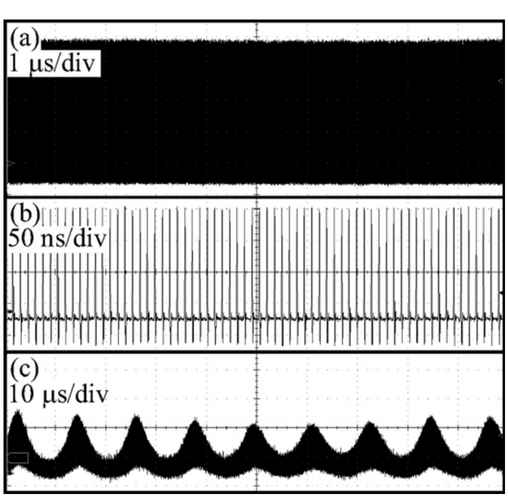

Fig. 2. Pulse trains of (a,b) cw mode-locking and (c) Q-switched mode-locking.

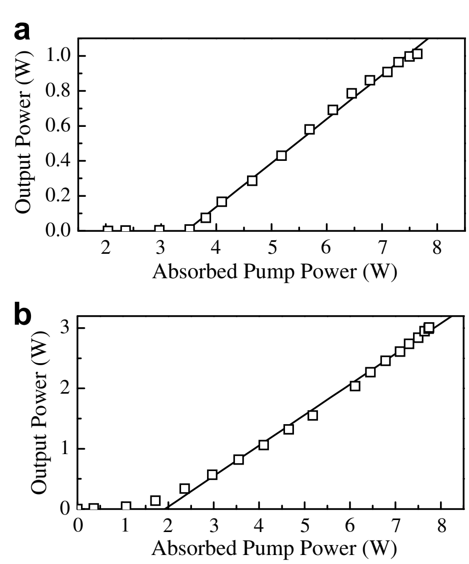

Fig. 3. Output power with respect to the absorbed pump power at (a) cw mode-locking operation compared to (b) cw operation with a two-mirror cavity setup.

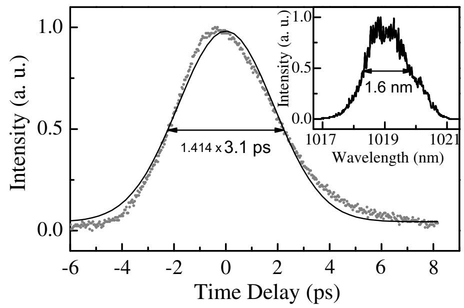

Fig. 4. Autocorrelation trace of the cw mode-locked pulses. Inset: the corresponding spectrum.

the pump threshold for establishing cw mode-locking mainly by (1) reducing laser mode size in crystal and on SESAM, (2) employing a SESAM with smaller modulation depth, and (3) using an output coupler with smaller output coupling to increase intracavity pulse energy. However, these methods may come at the expense of laser performance such as laser efficiency and output power level.

Fig. 4 shows the measured autocorrelation trace of the cw mode-locked pulses. From the autocorrelation trace, the pulse duration was estimated to be 3.1 ps at FWHM, assuming a Gaussian profile. The spectral bandwidth of the mode-locked pulses was 1.6 nm at FWHM, centered at wavelength of 1019.1 nm (Fig. 4, inset). The spectrum was measured with a resolution of 0.05 nm. According to the pulse duration and bandwidth, the pulses were 3.2 times transform-limited, which implies that further compression on pulse duration is possible by means of, e.g., dispersion compensation.

4. Conclusion

In conclusion, we have experimentally demonstrated stable high-power cw mode-locking of a diode pumped Yb:$GdVO_4$ crystal laser with the SESAM technique. Under an absorbed pump power of 7.6 W the output power of the laser attained to 1.01 W. The mode-locked pulses had duration of 3.1 ps at ∼1019 nm. To our knowledge, this is the first demonstration of passive mode-locking of Yb:$GdVO_4$ crystal. We believe that the mode-locking performance of the laser can be further improved when the crystal doping concentration is optimized and the pump diode wavelength could be matched with the peak absorption wavelength of the crystal. Nevertheless, our results clearly suggest that Yb:$GdVO_4$ could be a promising gain medium for the high-power ultrashort pulse generation at 1 μm.

Acknowledgements

This work was partly supported by the National Research Foundation Singapore (Grant NRF-CRP 200701) and the National Natural Science Foundation of China (Grant No. 60725418).

References

[1] J. Petit, B. Viana, P. Goldner, D. Vivien, P. Louiseau, B. Ferrand, Opt. Lett. 29 (2004) 833.
[2] A.A. Lagatsky, A.R. Sarmani, C.T.A. Brown, W. Sibbett, V.E. Kisel, A.G. Selivanov, I.A. Denisov, A.E. Troshin, K.V. Yumashev, N.V. Kuleshov, V.N. Matrosov, T.A. Matrosova, M.I. Kupchenko, Opt. Lett. 30 (2005) 3234.
[3] W.X. Li, H.F. Pan, L.E. Ding, H.P. Zeng, G.J. Zhao, C.F. Yan, L.B. Su, J. Xu, Opt. Express 14 (2006) 686.
[4] J.H. Liu, X. Mateos, H.J. Zhang, J.Y. Wang, M.H. Jiang, U. Grielmer, V. Petrov, Opt. Lett. 31 (2006) 2580.
[5] D. Jaque, J.C. Lagomacini, C. Jacinto, T. Catunda, Appl. Phys. Lett. 89 (2006) 121101.
[6] N. Coluccelli, G. Galzerano, L. Bonelli, A. Di Lieto, M. Tonelli, P. Laporta, Opt. Express 16 (2008) 2922.
[7] G.Q. Xie, D.Y. Tang, H.J. Zhang, J.Y. Wang, L.J. Qian, Opt. Express 16 (2008) 1686.
[8] G.Q. Xie, D.Y. Tang, L.M. Zhao, L.J. Qian, K. Ueda, Opt. Lett. 32 (2007) 2741.
[9] V.E. Kisel, A.E. Troshin, V.G. Shcherbitsky, N.V. Kuleshov, V.N. Matrosov, T.A. Matrosova, M.I. Kupchenko, Opt. Lett. 30 (2005) 1150.
[10] Y. Cheng, H.J. Zhang, Y.G. Yu, J.Y. Wang, X.T. Tao, J.H. Liu, V. Petrov, Z.C. Ling, H.R. Xia, M.H. Jiang, Appl. Phys. B: Lasers Opt. 86 (2007) 681.
[11] C. Honninger, R. Paschotta, F. Morier-Genoud, M. Moser, U. Keller, J. Opt. Soc. Am. B Opt. Phys. 16 (1999) 46.